ROBUST AND SWITCHED CONTROL DESIGN FOR ELECTRICAL STIMULATION OF LOWER LIMBS: A LINEAR ANALYSIS

Willian Ricardo Bispo Murbak Nunes*, Ricardo Gouveia Teodoro†, Rafael Augusto de Araujo‡, Marcelo Augusto Assunção Sanches‡, Marcelo Carvalho Minhoto Teixeira§, Aparecido Augusto de Carvalho‡

*UTFPR - Federal University of Technology - Paraná
Electrical Engineering Research Group
Marcilio Dias St., 635, 86812-460, Apucarana, PR, Brazil.

†IFPR - Federal Institute of Paraná
José Felipe Tequinha St., 1400
Paranavaí, Paraná, Brazil.

‡UNESP - São Paulo State University, Ilha Solteira Campus
Instrumentation and Biomedical Engineering Laboratory, Department of Electrical Engineering
José Carlos Rossi Ave., 1370, 15385-000, Ilha Solteira, SP, Brazil.

§UNESP - São Paulo State University, Ilha Solteira Campus
Control Research Laboratory, Department of Electrical Engineering
José Carlos Rossi Ave., 1370, 15385-000, Ilha Solteira, SP, Brazil.

Emails: willianr@utfpr.edu.br, ricardo.teodoro@ifpr.edu.br, rafael-feis@hotmail.com, sanches@dee.feis.unesp.br, marcelo@dee.feis.unesp.br, aac@dee.feis.unesp.br

Abstract— Functional electrical stimulation (FES) has been used to restore and aid motor functions in paraplegics, promoting better therapeutic results for its users. From experimental results, we observe that the control signal is uncertain for an operating point, because of plant uncertainties. We present an experimental setup to identify the linear model containing polytopic uncertainties, and design robust $p_{(r,\xi)}(t)$ and switched controller $p_{(\sigma,\xi)}(t)$ that compensate uncertain control signal through an adequate switching law. Results obtained from open-loop control p_0, robust controllers $p_r(t)$ and $p_{(r,\xi)}(t)$, and switched controllers $p_\sigma(t)$ and $p_{(\sigma,\xi)}(t)$ are compared. These results indicate that switched controller $p_{(\sigma,\xi)}(t)$ minimizes the uncertainty in the control signal, returns the smallest time derivative value of the Lyapunov function, consequently minimizing the angular position error in steady state ($e_{ss} \approx 0.20°$) in electrically stimulated lower limbs.

Keywords— Switched control, linear matrix inequalities (LMIs), rehabilitation, neuromuscular electrical stimulation.

Resumo— A estimulação elétrica funcional (FES) tem sido utilizada para restaurar e auxiliar as funções motoras em paraplégicos, promovendo melhores resultados terapêuticos. Por meio de resultados experimentais, foi observado que o sinal de controle é incerto para um ponto de operação, pois depende das incertezas da planta. Neste trabalho foi utilizado um aparato experimental para identificar o modelo linear contendo incertezas politópicas e então projetaram-se controladores robusto $p_{(r,\xi)}(t)$ e chaveado $p_{(\sigma,\xi)}(t)$ que compensam a incerteza no sinal de controle através de uma lei de chaveamento adequada. Resultados obtidos de malha aberta (p_0), controladores robustos $p_r(t)$ e $p_{(r,\xi)}(t)$, e chaveados $p_\sigma(t)$ e $p_{(\sigma,\xi)}(t)$, são comparados. Dentre as comparações, o melhor resultado se deu do controlador chaveado $p_{(\sigma,\xi)}(t)$ minimizou a incerteza no sinal de controle com o menor erro de posição angular em estado estacionário ($e_{ss} \approx 0.20°$), e retornou o menor valor de derivada da função de Lyapunov.

Palavras-chave— Controle chaveado, desigualdades matriciais lineares (LMI's), reabilitação, estimulação elétrica neuromuscular, FES.

1 Introduction

The functional electrical stimulation (FES) is a very promising technique to minimize muscle spasticity and assist in restoring the movements of paraplegic individuals.

Closed-loop control allows smoother stimulated limb movement. The system's mathematical model to be controlled is fundamental for the controllers design. In particular, the relationship between the voltage or current pulse width and the joint motion must be well understood. However, this process involves biomechanical interactions and several complex, nonlinear and uncertain physiological phenomena.

Currently, several control techniques have been applied. Downey et al. (2017) developed switching between stimulation channels. Rodor et al. (2017) proposed a PID with feedback error learning for position control. Da Mata et al. (2017) verified the robust H_∞ controller behavior to reject disturbances.

Other studies are worth discussing. Guaracy et al. (2016) designed a controller by *fuzzy* sliding modes, considering that there is repeatability and a linear relationship between pulse width and angular position. However, Guaracy et al. (2016)

supposition and also several other authors, does not correspond to the experimental reality since the lower limb movement has a non-linear, complex and uncertain dynamic behavior.

Covacic and Gaino (2014) presented an control design for strictly positive real (SPR) systems using polytopic uncertainties only in the characteristic matrix. In this paper, we analyze uncertainties in the state and input matrices.

In all previous studies, none has experimentally recognized that the control signal is uncertain. Through experimental results, we show that the control signal at an operating point is uncertain because it depends on the uncertainties of the plant. Unfortunately, this was not done in previous studies, since they used the identification parameters obtained by Ferrarin and Pedotti (2000) and validated the control technique in closed loop by simulation.

In this work, propose an experimental setup to identify the linear model containing polytopic uncertainties. FES involves repetitive stimulation of the muscle, which can lead to fatigue. An important contribution given in this paper is to show how to identify experimentally the uncertain parameters in the state space model. So it is possible to evaluate model parametric variation for non-fatigued and fatigued muscle conditions.

In addition, this study contributes to the analysis of an uncertain control signal, compares the performance of robust and switched controllers, and compensates uncertain control signal by a switched control law $p_{(\sigma,\xi)}(t)$.

The article is organized as follows: in section 2, the dynamic model in the state space considering polytopic uncertainties is presented; in section 3 describes the experimental protocol for polytopic uncertainties identification; in section 4 indicates the robust and switched control design for electrically stimulated lower limb considered as linear system in an operating point and results obtained; and section 5 concludes about results.

2 Modeling of the Lower Limb considering Polytopic Uncertainties

In a system that presents parametric uncertainties, these can be restricted by a convex linear combination belonging to the set described as polytope.

2.1 State-space model

Sanches (2013) in his study proposed a state-space model modification to facilitate practical implementation with accelerometers. Thus, the torque state variable was replaced by acceleration. Further details of this technique can be found in Sanches (2013).

In this paper, we consider the linear system with polytopic uncertainties given by:

$$\dot{\mathbf{x}}(t) = \mathbf{A}(\alpha)\mathbf{x}(t) + \mathbf{B}(\alpha)u(t), \quad (1)$$

$$\mathbf{y}(t) = \mathbf{C}\mathbf{x}(t), \quad (2)$$

being $\mathbf{A}(\alpha) \in \mathbb{R}^{nxn}$ the state matrix, $\mathbf{B}(\alpha) \in \mathbb{R}^{nxm}$ the input matrix, $\mathbf{x}(t) \in \mathbb{R}^n$ the state vector, $u(t) \in \mathbb{R}^m$ the input control, $\mathbf{y}(t) \in \mathbb{R}^q$ the output vector, and $\mathbf{C} \in \mathbb{R}^{qxn}$ the output matrix.

The system (1) and (2) can be described as a convex combination of the polytope vertices, with parameters belonging to the unitary simplex $\mathfrak{U}$:

$$\mathfrak{U} = \left\{ (\mathbf{A},\mathbf{B})(\alpha) : \sum_{i=1}^{r} \alpha_i (\mathbf{A},\mathbf{B})_i ; \sum_{i=1}^{r} \alpha_i = 1; \right. \\ \left. \alpha_i \geq 0; i \in \mathbb{Q}_r \right\}, \quad (3)$$

$$\mathbb{Q}_r = \{1, 2, \cdots, r\}. \quad (4)$$

Regarding to knee joint movement due to electrical stimulation applied in the quadriceps, the state-space representation (1) and (2) is given by:

$$\mathbf{A}(\alpha) = \begin{bmatrix} 0 & 1 & 0 \\ 0 & 0 & 1 \\ \tilde{\mathfrak{L}}(z) & \tilde{\mathfrak{I}}(z) & \mathfrak{E}(\tau) \end{bmatrix},$$

$$\mathbf{B}(\alpha) = \begin{bmatrix} 0 \\ 0 \\ \mathfrak{B}(G, \tau) \end{bmatrix},$$

$$\mathbf{C} = \begin{bmatrix} 1 & 0 & 0 \\ 0 & 1 & 0 \\ 0 & 0 & 1 \end{bmatrix},$$

where the state vector $\mathbf{x}(t) = \begin{bmatrix} x_1(t) & x_2(t) & x_3(t) \end{bmatrix}^T$, and the control input $u(t) = p_n(t)$, $z(t) = \begin{bmatrix} x_1(t) & \lambda & E & \omega \end{bmatrix}^T \in \mathbb{R}^4$; λ and E are coefficients of the exponential term related with movement stiffness; ω the elastic resting angle of the knee; G and τ are parameters that express the first-order relation of the torque and electric stimulus pulse width $p_n(t)$.

In relation to parameters and variables, we define that $x_1(t)$ is the angular position of the knee joint, $x_2(t)$ is the angular velocity, $x_3(t)$ is the angular acceleration.

For convenience of notation, all state variables will be considered as time-dependent, for example $x_1(t) = x_1$. When $x_1(t)$ is explicit, it will be to emphasize dependence in the time domain.

The system control input $p_n(t)$ at the equilibrium point is given by:

$$p_n(t) = p(t) - p_0, \quad (5)$$

where $p(t)$ is the pulse width in μsec, and p_0 is pulse width that produces active torque by the electrical stimulation at the desired operating point.

The vertices number of polytope is given by 2^s, where s is the uncertainties number. In this paper we adopt four uncertainties ($s = 4$), corresponding to a polytope composed of 16 vertices.

A linearized model obtained based on the results presented in Ferrarin and Pedotti (2000) and Sanches (2013) is presented in (6), so the model (1) is given by:

$$\begin{bmatrix} \dot{x}_1(t) \\ \dot{x}_2(t) \\ \dot{x}_3(t) \end{bmatrix} = \begin{bmatrix} 0 & 1 & 0 \\ 0 & 0 & 1 \\ l & i & e \end{bmatrix} \begin{bmatrix} x_1(t) \\ x_2(t) \\ x_3(t) \end{bmatrix} + \begin{bmatrix} 0 \\ 0 \\ b \end{bmatrix} p_n(t), \quad (6)$$

where l, i, e, and $b \in \mathbb{R}$ are uncertain parameters obtained experimentally.

3 Parameters Identification

3.1 Subjects

This study was authorized through a research ethics committee involving human beings (CAEE 79219317.2.1001.5402) in São Paulo State University (UNESP), Ilha Solteira campus. An able-bodied male subject, 26 years old, participated in the study.

3.2 Test plataform

Experiments were performed on a test platform shown in Figure 1. The platform is composed of a chair instrumented by an electrogoniometer (*Lynx*®), a gyroscope LPR510AL (*ST Microelectronics*®), two triaxial accelerometers MMA7341 (*Freescale*®), a NI myRIO controller (*National Instruments*®), a current-based neuromuscular electrical stimulator (more details can be found in Sanches (2013), and an user interface developed in the LabVIEW Student Edition. For

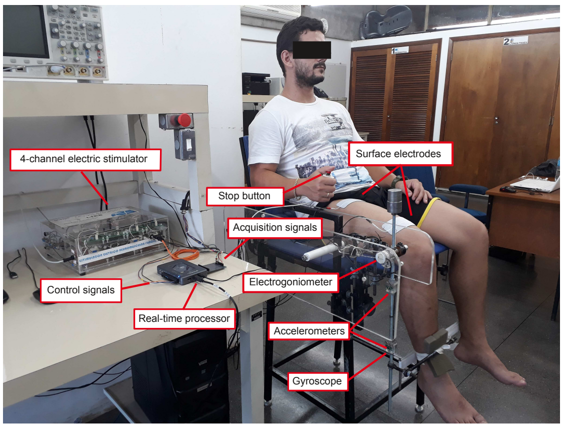

Figure 1: The leg extension machine was equipped with electrogoniometer, gyroscope and accelerometer to measure the angle, velocity and acceleration of the knee joint, respectively. From an embedded controller control signals are sent to the stimulator.

greater confidence and comfort of the volunteer, the patient can deactivates the stimulation pulses using a stop button. The chair backrest and the knee joint position are adjustable for each volunteer.

The stimulation intensity is controlled by setting the pulse amplitude to the quadriceps and controlling the pulse width. The stimulus frequency were fixed in 50 Hz. In a preliminary test, pulse amplitude was determined at about 70 mA. The muscular electrostimulator delivers rectangular, biphasic, symmetrical pulse to the individual's muscle, and allows an adjustment of the pulse width in a range of 0-500 μs.

3.3 Experimental setup

Before applying the stimuli to the quadriceps, a muscle analysis determines the motor point for proper positioning of the surface electrodes. Then, scraping and cleansing procedures are performed at the motor point. The electrodes used are rectangular self-adhesive CARCI 50 mm x 90 mm.

After the motor-point identification, open-loop experimental tests are performed. The open-loop test consists of applying a step-type signal corresponding to a constant pulse width p_0. The test duration is about four seconds. Thereafter, approximately 2-minutes time interval is timed for muscle rest. After the rest period, the step-type test is applied again for four seconds.

The pulse width, position, velocity and angular acceleration data are automatically recorded at the end of the step-type signal.

At each test the measured angular position should be the closest to the desired position. However, after several tests applied sequentially it is noticeable that the measured angular position tends to be more divergent from the desired angular position, Figure 2. Note that after a large number of tests the error becomes very large. Our hypothesis is that the muscle fibers recruited locally by the surface electrodes are saturated which leads to the fatigue state. The criterion used to determine the saturation condition of the fibers was defined by the evaluation of the error obtained between the desired and measured position. With an relative error greater than 15-20%, the test results are referred to as fatigued situation for identification at an operating point $\mathbf{x}_0$.

After a day of several tests, we observed a early fatigue in the muscles. Therefore, about 24 hours after, muscular behavior was evaluated again for step-type signals. In these trials the obtained results were referred as fatigued situation, Figure 2.

3.4 Vertices of the Polytope

The experimental data were processed via MATLAB. The parameters values of the identification sets (non-fatigued and fatigued) are shown in the

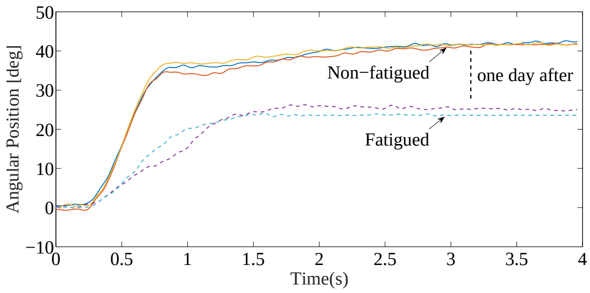

Figure 2: Parameters identification test for the model (6), performed by the successive application of step-type signals interspersed 2 minutes and considering a one-day interval between fatigued and non-fatigued run.

Table 1 and vertices of the polytope $(A_i,\ B_i)$, given by:

$$\mathbf{A}_1 = \mathbf{A}_2 = \begin{bmatrix} 0 & 1 & 0 \\ 0 & 0 & 1 \\ l_{min} & i_{min} & e_{min} \end{bmatrix},$$

$$\mathbf{A}_3 = \mathbf{A}_4 = \begin{bmatrix} 0 & 1 & 0 \\ 0 & 0 & 1 \\ l_{min} & i_{min} & e_{max} \end{bmatrix},$$

$$\mathbf{A}_5 = \mathbf{A}_6 = \begin{bmatrix} 0 & 1 & 0 \\ 0 & 0 & 1 \\ l_{min} & i_{max} & e_{min} \end{bmatrix},$$

$$\mathbf{A}_7 = \mathbf{A}_8 = \begin{bmatrix} 0 & 1 & 0 \\ 0 & 0 & 1 \\ l_{min} & i_{max} & e_{max} \end{bmatrix},$$

$$\mathbf{A}_9 = \mathbf{A}_{10} = \begin{bmatrix} 0 & 1 & 0 \\ 0 & 0 & 1 \\ l_{max} & i_{min} & e_{min} \end{bmatrix},$$

$$\mathbf{A}_{11} = \mathbf{A}_{12} = \begin{bmatrix} 0 & 1 & 0 \\ 0 & 0 & 1 \\ l_{max} & i_{min} & e_{max} \end{bmatrix},$$

$$\mathbf{A}_{13} = \mathbf{A}_{14} = \begin{bmatrix} 0 & 1 & 0 \\ 0 & 0 & 1 \\ l_{max} & i_{max} & e_{min} \end{bmatrix},$$

$$\mathbf{A}_{15} = \mathbf{A}_{16} = \begin{bmatrix} 0 & 1 & 0 \\ 0 & 0 & 1 \\ l_{max} & i_{max} & e_{max} \end{bmatrix},$$

$$\mathbf{B}_1 = \mathbf{B}_3 = \mathbf{B}_5 = \cdots = \mathbf{B}_{15} = \begin{bmatrix} 0 \\ 0 \\ b_{min} \end{bmatrix},$$

$$\mathbf{B}_2 = \mathbf{B}_4 = \mathbf{B}_8 = \cdots = \mathbf{B}_{16} = \begin{bmatrix} 0 \\ 0 \\ b_{max} \end{bmatrix}.$$

Table 1: Parameters values of the model, eq. (6).

	Non-fatigued		Fatigued	
	min	max	min	max
l	-104,8630	-45,5413	-53,6807	-18,9582
i	-55,2046	-34,4644	-35,1242	-15,5393
e	-6,3065	-5,0064	-8,6351	-5,6134
b	0,1111	0,2516	0,0279	0,0738

4 Robust and Switched Control Design

The control technique used in this work is derived from De Souza et al. (2013). We assume an analysis of the system around a point of equilibrium $\bar{\mathbf{x}}(t) = \mathbf{x}_0$, so a linearization can be applied to the plant $\dot{\bar{\mathbf{x}}}(t) = f\left(\bar{\mathbf{x}}(t), \bar{p}(t)\right)$, and control input $\bar{p}(t) = p_0$. Consider that $\mathbf{x}_0$ is known, p_0 is uncertain because it depends on the plant uncertainties, but

$$\mathfrak{D} = \left\{p_0 \in \mathbb{R}_+^*; p_{0min} < p_0 < p_{0max}\right\}, \tag{7}$$

where p_{0min} and p_{0max} are known.

Thus, we considered in this paper the linearized system given by:

$$\dot{\mathbf{x}}(t) = \mathbf{A}(\alpha)\mathbf{x}(t) + \mathbf{B}(\alpha)p(t), \tag{8}$$

such that $\mathbf{x}(t) = \bar{\mathbf{x}}(t) - \mathbf{x}_0$, $\bar{\mathbf{x}}(t)$ is the state vector of the plant, $p_n(t) = \bar{p}(t) - p_0$, $p(t)$ is the control signal, $\mathbf{B}(\alpha) = \mathbf{B}g(\alpha)$, $\mathbf{B}$ is a constant matrix, and the bounded function $g(\alpha) \in \mathbb{R}_+^*$, that depends on uncertain parameters α.

Considering for all α given in (3), so the system linearized (8) can be rewritten as:

$$\dot{\mathbf{x}}(t) = \mathbf{A}(\alpha)\mathbf{x}(t) + \mathbf{B}g(\alpha)p(t). \tag{9}$$

where $\mathbf{B}$ is a constant, and $g(\alpha) > 0$.

In this paper, consider two state-feedback control law. The first control law is classical for the robust controller, given by:

$$\bar{p}(t) = \bar{p}_r(t) = -\mathbf{K}_r x(t), \tag{10}$$

where $\mathbf{K}_r \in \mathbb{R}^{mxn}$. Replacing (10) in (9), one obtains the feedback system:

$$\begin{aligned} \dot{\mathbf{x}}(t) &= \mathbf{A}(\alpha)\mathbf{x}(t) - \mathbf{B}(\alpha)\mathbf{K}_r\mathbf{x}(t), \\ &= \sum_{i=1}^{r} \alpha_i \left(\mathbf{A}_i - \mathbf{B}_i\mathbf{K}_r\right)\mathbf{x}(t), \end{aligned} \tag{11}$$

The second feedback control law is specified for switched controller given by:

$$\bar{p}(t) = \bar{p}_\alpha(t) = -\sum_{i=1}^{r} \alpha_i \mathbf{K}_i x(t) = -\mathbf{K}(\alpha)\mathbf{x}(t), \tag{12}$$

where $\mathbf{K}_i \in \mathbb{R}^{mxn}$, $i \in \mathbb{Q}_r$. Considering (12) and from (3) and (9),

$$\begin{aligned} \dot{\mathbf{x}}(t) &= \mathbf{A}(\alpha)\mathbf{x}(t) - \mathbf{B}(\alpha)\mathbf{K}(\alpha)\mathbf{x}(t), \\ &= \sum_{i=1}^{r}\sum_{j=1}^{r} \alpha_i\alpha_j \left(\mathbf{A}_i - \mathbf{B}_i\mathbf{K}_j\right)\mathbf{x}(t), \end{aligned} \tag{13}$$

Besides the stability, it is desired guarantee other performance indices for the controlled system, such as the setting time, norm constraint and others. The setting time is related to the decay rate of the system.

4.1 Stability + Decay Rate

Theorem 1 *Boyd et al. (1994) - The linear system with polytopic uncertainties given in* (11) *is quadratically stabilizable, with decay rate greater than or equal to* β*, if and only if there exist a symmetric positive definite matrix* $\boldsymbol{X}$ *and* $\boldsymbol{M} \in \mathbb{R}^{m\times n}$ *such that, for all* $i \in \mathbb{Q}_r$*, the following LMIs hold:*

$$\boldsymbol{X}\boldsymbol{A}_i^T + \boldsymbol{A}_i\boldsymbol{X} - \boldsymbol{B}_i\boldsymbol{M} - \boldsymbol{M}^T\boldsymbol{B}_i^T + 2\beta\boldsymbol{X} < 0, \quad (14)$$

If there exists such a solution, the controller gain is given by $\boldsymbol{K}_r = \boldsymbol{M}\boldsymbol{X}^{-1}$ *and* $\boldsymbol{P}_r = \boldsymbol{P} = \boldsymbol{X}^{-1}$.

Proof: The proof is detailed in Boyd et al. (1994), considering $\dot{V}(\mathbf{x}) \leq -2\beta V(\mathbf{x})$. □

Theorem 2 *De Souza et al. (2013) - The equilibrium point* $\mathbf{x} = 0$ *of the linear system with polytopic uncertainties given in* (13) *is asymptotically stable in the large, with decay rate greater than or equal to* β*, if there exist a common symmetric positive definite matrix* $\boldsymbol{X}$ *and* $\boldsymbol{M}_i \in \mathbb{R}^{m\times n}$ *such that, for all* $i, j \in \mathbb{Q}_r$*, the following LMIs hold:*

$$\boldsymbol{X}\boldsymbol{A}_i^T + \boldsymbol{A}_i\boldsymbol{X} - \boldsymbol{B}_i\boldsymbol{M}_i - \boldsymbol{M}_i^T\boldsymbol{B}_i^T + 2\beta\boldsymbol{X} < 0, \quad (15)$$

$$(\boldsymbol{A}_i + \boldsymbol{A}_j)\boldsymbol{X} + \boldsymbol{X}(\boldsymbol{A}_i + \boldsymbol{A}_j)^T - \boldsymbol{B}_i\boldsymbol{M}_j - \boldsymbol{B}_j\boldsymbol{M}_i - \boldsymbol{M}_i^T\boldsymbol{B}_j^T - \boldsymbol{M}_j^T\boldsymbol{B}_i^T + 4\beta\boldsymbol{X} \leq 0, i < j \quad (16)$$

If (15) *and* (16) *are feasible, the controller gains are given by* $\boldsymbol{K}_i = \boldsymbol{M}_i\boldsymbol{X}^{-1}$, $i \in \mathbb{Q}_r$*, and* $\boldsymbol{P} = \boldsymbol{X}^{-1}$.

Proof: The proof is similar to that of Theorem 1. □

4.2 Norm Constraint

One can constraint the norm of the controller gains by imposing restrictions on $\mathbf{M}_i$, $i \in \mathbb{K}_r$, and $\mathbf{X}^{-1}$ as in Šiljak and Stipanovic (2000). Thus, given the constants $\eta > 0$ and $\eta_x > 0$, imposing that $\mathbf{M}_i^T\mathbf{M}_i < \eta\mathbf{I}_n$, $i \in \mathbb{K}_r$ and $\mathbf{X}^{-1} < \eta_x\mathbf{I}_x$, then a constraint on the controller gains may be established by the following theorem.

Theorem 3 *Šiljak and Stipanovic (2000) - The constraint on the norm of the controller gains such that* $\boldsymbol{K}_i\boldsymbol{K}_i^T \leq \eta\eta_x^2\boldsymbol{I}_m$, $i \in \mathbb{K}_r$ *is enforced if there exist constants* $\eta > 0$ *and* $\eta_x > 0$*, such that the LMIs from Theorems 2 or 1 (replacing* $\boldsymbol{K}_i = K$ *and* $\boldsymbol{M}_i = M$*), with the LMIs below hold:*

$$\begin{bmatrix} \eta_x\boldsymbol{I}_n & \boldsymbol{I}_n \\ \boldsymbol{I}_n & \boldsymbol{X} \end{bmatrix} \geq 0, \begin{bmatrix} \eta\boldsymbol{I}_n & \boldsymbol{M}_i^T \\ \boldsymbol{M}_i & \boldsymbol{I}_m \end{bmatrix} \geq 0, \quad (17)$$

Proof: The proof is detailed in Šiljak and Stipanovic (2000). □

4.3 Robust and Switched control law for uncertainty in the control signal

Assume that the robust gain $\mathbf{K}_r = \mathbf{M}\mathbf{X}^{-1}$, and the matrix $\mathbf{P}_r = \mathbf{X}^{-1}$, have been obtained using the vertices of the polytope of the system (8) in the LMIs from Theorem 1. Now, given a constant ξ, define the switched control law:

$$p_n(t) = p_{n(r,\xi)}(t) = \bar{p}_{(r,\xi)}(t) - p_0, \quad (18)$$

with

$$\bar{p}_{(r,\xi)}(t) = -\mathbf{K}_r\mathbf{x}(t) + \gamma_\xi(t). \quad (19)$$

Moreover, assume that the gains $\mathbf{K}_i = \mathbf{M}_i\mathbf{X}^{-1}$, $i \in \mathbb{Q}_r$ and the matrix $\mathbf{P} = \mathbf{X}^{-1}$, have been obtained using the vertices of the polytope of the system (8) in the LMIs from Theorem 2. Now, given a constant ξ, define the switched control law:

$$p_n(t) = p_{n(\sigma,\xi)}(t) = \bar{p}_{(\sigma,\xi)}(t) - p_0, \quad (20)$$

with

$$\bar{p}_{(\sigma,\xi)}(t) = -\mathbf{K}_\sigma\mathbf{x}(t) + \gamma_\xi(t), \quad (21)$$

where

$$\mathbf{K}_\sigma \in \{K_1, K_2, \cdots, K_r\},$$
$$\sigma = \arg\min_{i\in\mathbb{K}_r} \left\{-\mathbf{x}^T\mathbf{P}\mathbf{B}\mathbf{K}_i\mathbf{x}\right\}.$$

In both controllers the switching law $\gamma_\xi(t)$ is defined by:

$$\gamma_\xi(t) = \begin{cases} p_{0max}, & \text{if } \mathbf{x}^T\mathbf{P}\mathbf{B}(t) < -\xi \\ p_l, & \text{if } \left|\mathbf{x}^T\mathbf{P}\mathbf{B}(t)\right| \leq \xi \\ p_{0min}, & \text{if } \mathbf{x}^T\mathbf{P}\mathbf{B}(t) > \xi \end{cases}, \quad (22)$$

where $p_l = \left[(p_{0min} - p_{0max})\,\mathbf{x}^T\mathbf{P}\mathbf{B}(t)\right](2\xi)^{-1} + p_0$.

Consider the index $\Xi(t) \in \mathbb{Z}$, as the signal switching state $\gamma_\xi(t)$:

$$\Xi(t) = \begin{cases} 1, & \text{if } \mathbf{x}^T\mathbf{P}\mathbf{B}(t) > \xi \\ 2 & \text{if } \left|\mathbf{x}^T\mathbf{P}\mathbf{B}(t)\right| \leq \xi \\ 3, & \text{if } \mathbf{x}^T\mathbf{P}\mathbf{B}(t) < -\xi \end{cases}. \quad (23)$$

Theorem 4 *Suppose that the conditions from Theorem 1 hold, from the system* (8) *with the control law* (10) *and obtain* $\boldsymbol{K}_r = \boldsymbol{M}\boldsymbol{X}^{-1}$*, and* $\boldsymbol{P}_r = \boldsymbol{X}^{-1}$*. Then, the robust control law* (18)*,* (19)*, and* (22) *makes the system* (8) *uniform ultimate bounded.*

Theorem 5 *De Souza et al. (2013)- Suppose that the conditions from Theorem 2 hold, from the system* (8) *with the control law* (12) *and obtain* $\boldsymbol{K}_i = \boldsymbol{M}_i\boldsymbol{X}^{-1}$, $i \in \mathbb{Q}_r$*, and* $\boldsymbol{P} = \boldsymbol{X}^{-1}$*. Then, the switched control law* (20)*,* (21)*, and* (22) *makes the system* (8) *uniform ultimate bounded.*

Proof: The proof is detailed in De Souza et al. (2013). □

The solutions of the LMIs for the design of the gains of the controllers were carried out using the modelling language YALMIP (Lofberg (2004)) with the solver SeDuMi(Sturm (1999)).

For the robust and switched controllers, we adopted the norm constraint $\eta = 600$ and $\eta_x = 30$,and decay rate $\beta = 0.5$. The following symmetric positive matrix $\mathbf{P}_r$ and gains $\mathbf{K}_r$ were obtained for the robust controller:

$$\mathbf{P}_r = \begin{bmatrix} 28.7796 & 5.3481 & 0.4551 \\ 5.3481 & 2.5941 & 0.1872 \\ 0.4551 & 0.1872 & 0.0534 \end{bmatrix},$$

$$\mathbf{K}_r = \begin{bmatrix} 80.8672 & 52.1583 & 4.0207 \end{bmatrix}.$$

While that for the switched controller, the following symmetric positive matrix $\mathbf{P}$ and gains $\mathbf{K}_i$ were obtained:

$$\mathbf{P} = \begin{bmatrix} 8.7724 & 1.3997 & 0.1548 \\ 1.3997 & 0.6004 & 0.0495 \\ 0.1548 & 0.0495 & 0.0149 \end{bmatrix},$$

$$\mathbf{K}_1 = \begin{bmatrix} -7.4958 & -0.5771 & -0.0518 \end{bmatrix},$$

$$\mathbf{K}_2 = \begin{bmatrix} -32.5384 & -4.8576 & -0.5143 \end{bmatrix},$$

$$\mathbf{K}_3 = \begin{bmatrix} -207.9231 & -35.8229 & -3.8138 \end{bmatrix},$$

$$\mathbf{K}_4 = \begin{bmatrix} -139.8365 & -25.1311 & -2.5777 \end{bmatrix},$$

$$\mathbf{K}_5 = \begin{bmatrix} 158.8758 & 29.8286 & 3.1164 \end{bmatrix},$$

$$\mathbf{K}_6 = \begin{bmatrix} 126.9480 & 25.1264 & 2.5832 \end{bmatrix},$$

$$\mathbf{K}_7 = \begin{bmatrix} 91.5987 & 23.3575 & 2.2327 \end{bmatrix},$$

$$\mathbf{K}_8 = \begin{bmatrix} 49.8391 & 15.3702 & 1.4101 \end{bmatrix},$$

$$\mathbf{K}_9 = \begin{bmatrix} 157.0941 & 25.8703 & 2.8435 \end{bmatrix},$$

$$\mathbf{K}_{10} = \begin{bmatrix} 139.4140 & 22.7201 & 2.5133 \end{bmatrix},$$

$$\mathbf{K}_{11} = \begin{bmatrix} 109.7619 & 12.4137 & 1.6724 \end{bmatrix},$$

$$\mathbf{K}_{12} = \begin{bmatrix} 86.9418 & 9.2396 & 1.3009 \end{bmatrix},$$

$$\mathbf{K}_{13} = \begin{bmatrix} 213.4855 & 36.5931 & 3.9388 \end{bmatrix},$$

$$\mathbf{K}_{14} = \begin{bmatrix} 189.4155 & 32.7910 & 3.5200 \end{bmatrix},$$

$$\mathbf{K}_{15} = \begin{bmatrix} 197.7200 & 34.2314 & 3.6752 \end{bmatrix},$$

$$\mathbf{K}_{16} = \begin{bmatrix} 182.0206 & 31.7998 & 3.4064 \end{bmatrix}.$$

In relation to the control law (22), the maximum and minimum values of p_0 must be find. However, these values can not be determined analytically. So, we define these values by means of the experimental results obtained in the section parameters identification:

$$\max\{p_0\} = 350\mu sec, \tag{24}$$

$$\min\{p_0\} = 250\mu sec. \tag{25}$$

For the numerical simulation, at $t = 0s$ it considered the initial condition $\bar{\mathbf{x}}(0) = \begin{bmatrix} 0^\circ & 0 & 0 \end{bmatrix}$, and $p_0 = 300\mu s$. It is emphasized that the angular position state x_1 is given in rad, but the value shown in the Figure 3 is degrees. In $t = 2s$, from Figure 3, the system stabilizes in the desired position $\bar{\mathbf{x}}(2) = \begin{bmatrix} 42^\circ & 0 & 0 \end{bmatrix}$. From $t \in [10 \quad 20)\,s$ and $t \in [25 \quad 40]\,s$ the p_0 value of the system is purposely altered in order to compare the robust and switched controllers. During the time interval $t \in [10 \quad 15]\,s$ the p_0 value increases linearly and remains constant equal to $350\mu s$ until $t = 20s$. Note that the tendency of the leg position is to decline, corresponding to fatigued situations. In $t \in [20 \quad 25)\,s$ the value of p_0 returns to nominal $p_0 = 300\mu$s. In $t \in [25 \quad 30]\,s$ the value of p_0 decreases linearly and remains constant equal to $250\mu s$ until $t = 40s$. Now the tendency of the leg position is to rise, corresponding to the non-fatigued situations. This situation explains because the same pulse width of the controller does not give repeatability for leg position control. The results show that the $p_{(r,\xi)}(t)$ and $p_{(\sigma,\xi)}(t)$ controllers presented good compensation of the uncertain control signal.

An interesting analysis is to verify the details of the system operation for the uncertain control signal compensation (Figure 4). In open-loop the position error in steady-state (e_{ss}) is equal to 15.83°, while that robust $p_r(t)$ and switched $p_{(\sigma,\xi)}(t)$ controllers were 10.94° and 7.26°, respectively. We obtained the smallest error by including the switching law (22), so that for the robust and switched controllers were 0.36° and 0.20°, respectively.

The control law uses the signal $\mathbf{x}^T\mathbf{PB}(t)$ as a decision variable. The control signal uncertainty is evident in $\mathbf{x}^T\mathbf{PB}(t)$. By setting a given ξ which minimizes uncertainty, makes the system uniform ultimate bounded. Thus, it is explicit from the Figure 4 that the controller with $\gamma_\xi(t)$ law is more efficient than the one commonly used in the literature. The switched controller $p_{(\sigma,\xi)}(t)$ returned the smallest time derivative value of the Lyapunov function. It is worth mentioning that if the value ξ tending to zero, it will make the function $\gamma_\xi(t)$ discontinue and consequently the control signal will be discontinuous, causing chattering as shown in Figure 4.

5 Conclusions

This paper investigated the uncertain control signal problem involving electrical stimulation of lower limbs. The study focused on a linear analysis around an operating point. Experimental data were obtained for the identification of the polytopic linear model. A comparison between open-loop control and four closed-loop controllers. The switched controller $p_{(\sigma,\xi)}(t)$ returned the smallest

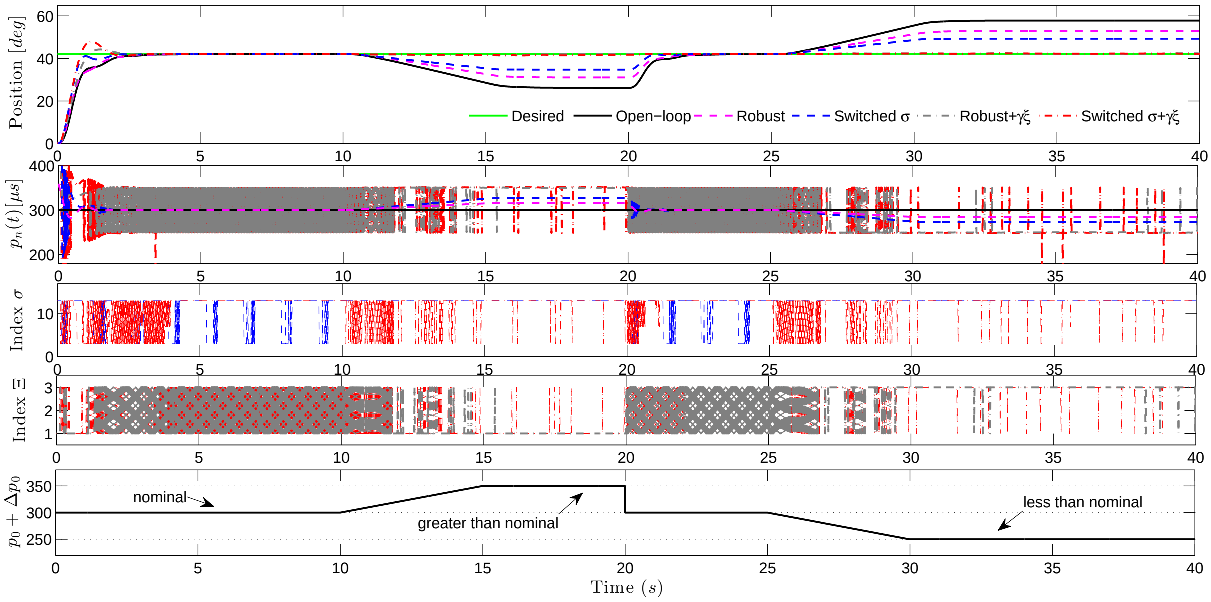

Figure 3: Dynamic behavior of lower limb electrical stimulation around an operating point (42°) with uncertain control signal. Considering decay rate $\beta = 0.5$, norm constraint $\eta = 600$ and $\eta_x = 30$, nominal pulsewidth $p_0 = 300\mu s$, $\xi = 1\text{x}10^{-7}$, and variation analysis of the uncertain control signal $\Delta p_0 = \pm 16,67\%$.

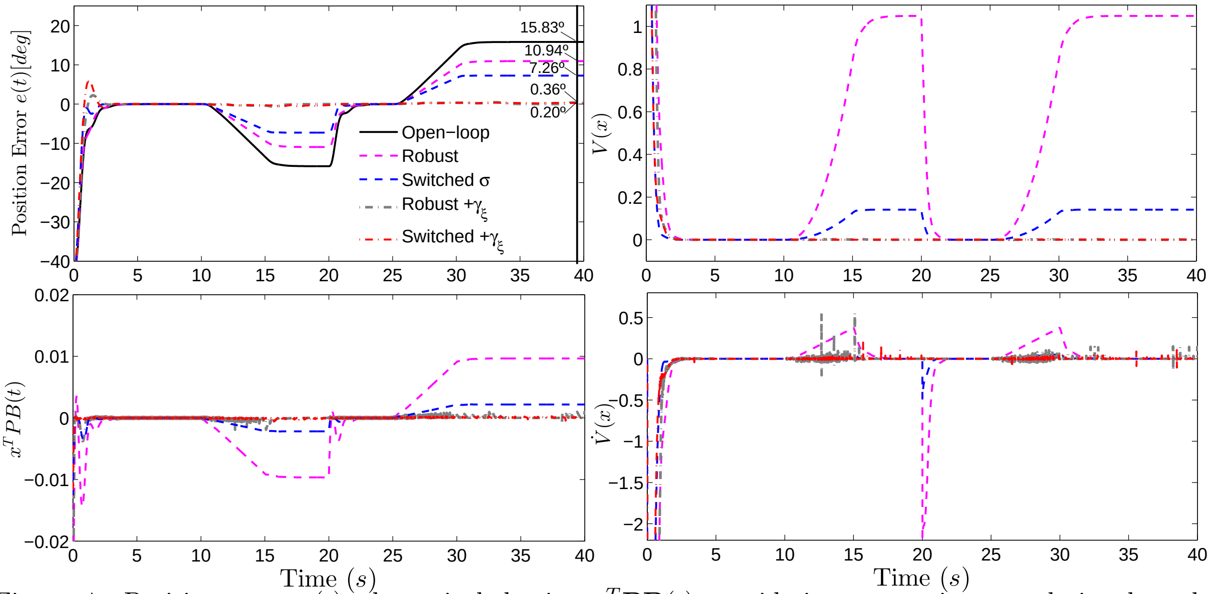

Figure 4: Position error $e(t)$, dynamic behavior $\mathbf{x}^T\mathbf{PB}(t)$ considering uncertain control signal, and Lyapunov function $V(\mathbf{x})$ and time-derivative $\dot{V}(\mathbf{x})$.

time derivative value of the Lyapunov function and compensated the uncertainty in the control signal.

Acknowledgments

The authors would like to thank the Brazilian agencies CAPES and CNPq which have supported this research.

References

Boyd, S., El Ghaoui, L., Feron, E. and Balakrishnan, V. (1994). *Linear matrix inequalities in system and control theory*, Vol. 15, SIAM, USA.

Covacic, M. R. and Gaino, R. (2014). Sistemas erp com funções de lyapunov variantes no tempo com aplicação em estimulação, *XX Congresso Brasileiro de Automática-CBA*, pp. 3357–3564.

Da Mata, D. A., Pereira, R. L., Pugliese, L. F. and

Kozan, R. F. (2017). Avaliação experimental de um controlador h_∞ para movimentar membros inferiores via estimulação elétrica funcional, *XIII Simpósio Brasileiro de Automação Inteligente-SBAI*, pp. 2247–2252.

De Souza, W. A., Teixeira, M. C. M., Santim, M., Cardim, R. and Assunção, E. (2013). On switched control design of linear time-invariant systems with polytopic uncertainties, *Mathematical Problems in Engineering* **2013**.

Downey, R. J., Cheng, T.-H., Bellman, M. J. and Dixon, W. E. (2017). Switched tracking control of the lower limb during asynchronous neuromuscular electrical stimulation: Theory and experiments, *IEEE Transactions on Cybernetics* **47**(5): 1251–1262.

Ferrarin, M. and Pedotti, A. (2000). The relationship between electrical stimulus and joint torque: A dynamic model, *IEEE Transactions on Rehabilitation Engineering* **8**(3): 342–352.

Guaracy, F. H. D., De Paula, C. F., Pereira, R. L. and Kozan, R. F. (2016). Controle do movimento dos membros inferiores por estimulação elétrica funcional via controlador por modos deslizantes fuzzy, *XXI Congresso Brasileiro de Automática-CBA*, pp. 104–109.

Lofberg, J. (2004). Yalmip: A toolbox for modeling and optimization in matlab, *Computer Aided Control Systems Design, 2004 IEEE International Symposium on*, IEEE, pp. 284–289.

Rodor, F. F., Pugliese, L. F., Pereira, R. L., Guaracy, F. H. D. and Kozan, R. F. (2017). Controle de posição da perna de pessoas hígidas utilizando feedback error learning, *XIII Simpósio Brasileiro de Automação Inteligente-SBAI*, pp. 1184–1189.

Sanches, M. A. A. (2013). Sistema eletrônico para geração e avaliação de movimentos em paraplégicos. PhD Thesis, Universidade Estadual Paulista (UNESP), São Paulo, Brazil.

Šiljak, D. and Stipanovic, D. (2000). Robust stabilization of nonlinear systems: the lmi approach, *Mathematical Problems in Engineering* **6**(5): 461–493.

Sturm, J. F. (1999). Using sedumi 1.02, a matlab toolbox for optimization over symmetric cones, *Optimization Methods and Software* **11**(1-4): 625–653.